Eric Lifshin (Ed.)

X-ray Characterization of Materials

WILEY-VCH

Weinheim · New York · Chichester · Brisbane · Singapore · Toronto

The page is intensily left blank

Related titles from WILEY-VCH

S. Amelinckx, D. van Dyck, J. van Landuyt, G. van Tendeloo (Eds.)
Handbook of Microscopy
3 Vols., ISBN 3-527-29444-9

S. N. Magonov, M.-U. Whangbo
Surface Analysis with STM and AFM
ISBN 3-527-29313-2

D. Brune, R. Hellborg, H. J. Whitlow, O. Hunderi
Surface Characterization
ISBN 3-527-28843-0

Eric Lifshin (Editor)

X-ray Characterization of Materials

WILEY-VCH

Eric Lifshin (Ed.)

X-ray Characterization of Materials

WILEY-VCH

Weinheim · New York · Chichester · Brisbane · Singapore · Toronto

Editor:
Dr. Eric Lifshin
Characterization and Environmental
Technology Laboratory
GE Corporate Research and Technology
1 Research Circle
Niskayuna, NY 12309
USA

Library of Congress Card No. applied for.

A catalogue record for this book is available from the British Library.

Deutsche Bibliothek Cataloguing-in-Publication Data:
X-ray characterization of materials / Eric Lifshin (ed.). Robert L.
Snyder ... – Weinheim ; New York ; Chichester ; Brisbane ; Singapore
; Toronto : Wiley-VCH, 1999
ISBN 3-527-29657-3

Printed on acid-free and chlorine-free paper.

Composition, Printing and Bookbinding: Konrad Triltsch, Druck- und Verlagsanstalt GmbH, D-97070 Würzburg
Printed in the Federal Republic of Germany

Preface

It is now just over 100 years since W. C. Roentgen (1898) first discovered x-rays. His work followed by that of H. G. Mosely (1912), W. L. and W. H. Bragg (1913), and other pioneers led the way to the development of many techniques essential to the characterization of metals, ceramics, semiconductors, glasses, minerals and biological materials. X-ray diffraction, fluorescence and absorption methods provide both qualitative and quantitative information about structure and composition essential to understanding material behavior. These methods are not only used in the course of basic research, but are also critical to the development of new materials required by society as well as understanding why materials fail in service. X-ray equipment is now found in laboratories all over including facilities that support steel mills, art museums, semiconductor fabrication facilitics to cite just a few examples. Although it is not the main focus of this volume, many major advances in medicine can be linked to the findings of x-ray crystallography and various forms of radiography. Today, three-dimensional reconstruction of the human body is possible in minutes utilizing the latest in computerized tomographic clinical instrumentation.

The ability to do such remarkable diagnostic work is the result of the continuing evolution of x-ray science and technology that has drawn heavily on advances in electronics, materials science, mechanical engineering and computers. As a result, x-ray generators are more stable, tubes capable of much higher intensities, spectrometers more versatile and accurate, and detectors and associated electronics are more sensitive and capable of higher count rates. Most modern instruments also incorporate some degree of automation making control of instruments and unattended collection of data possible. A wide range of software is also readily available for phase and elemental identification, determination of strain, texture measurement, particle size distribution, single crystal structure and thin film characterization. Both commercial and "home-made" x-ray instrumentation can be found in every major industrial, academic and government laboratory.

Progress does stop, however, and over the past few decades there has been even greater interest in x-ray methods arising from the use of multi-user synchrotron facilities that provide very intense sources of radiation. Synchrotron laboratories have opened the door to the practical application of a wide variety of additional characterization techniques including x-ray absorption fine structure (EXAFS), x-ray topography and both micro-scale x-ray fluorescence and diffraction. EXAFS, for example, provides information about local atomic environments and is particularly useful in the study of catalysts even those present in concentrations below hundreds of parts per million.

This volume also covers small angle x-ray scattering (SAX), a method that can be performed with either conventional or synchrotron sources. Data obtained at low angles is indicative of grain size and shape, i.e. structure with slightly larger dimensions than atomic separation distances, which are difficult to determine in other ways. An excellent example is the determination of the radius of gyration as a function of molecular weight for polymers. Other examples include studies of phase separation in alloy systems.

The authors of the various articles present are all experts in their fields. They have done an excellent job of acquainting readers with the history, underlying principals, instrumentation, capabilities and limitations of x-ray methods as well as numerous examples of their use, and have also suggested related reading. I think all readers will find this volume a unique source of information.

Eric Lifshin
Voorheeseville, NY
5/10/99

List of Contributors

Dr. Andrea R. Gerson
University of London
Department of Chemistry
King's College
The Strand
London WC2R 2LS
UK

Dr. André Guinier
Université de Paris-Sud
Laboratoire de Physique des Solides
F-91405 Orsay Cedex
France

Dr. Peter J. Halfpenny
University of Strathclyde
Department of Pure and Applied Chemistry
295 Cathedral Street
Glasgow G1 1XL
Scotland

Dr. Ronald Jenkins
JCPDS
International Centre for Diffraction Data
1601 Park Lane
Swarthmore, PA 19801-2389
USA

Dr. Roland P. May
Institut Laue-Langevin
Avenue des Martyrs 156X
F-38042 Grenoble Cedex 9
France

Dr. Stefania Pizzini
Centre Universitaire Paris-Sud
LURE
Bâtiment 209 D
F-91405 Orsay Cedex
France

Dr. Radoljub Ristic
University of Strathclyde
Department of Pure and Applied Chemistry
295 Cathedral Street
Glasgow G1 1XL
Scotland

Dr. Kevin J. Roberts
SERC Daresbury Laboratory
Warrington WA4 4AD
UK

Dr. David B. Sheen
University of Strathclyde
Department of Pure and Applied Chemistry
295 Cathedral Street
Glasgow G1 1XL
Scotland

Professor John N. Sherwood
University of Strathclyde
Department of Pure and Applied Chemistry
295 Cathedral Street
Glasgow G1 1XL
Scotland

Prof. Robert L. Snyder
Department of Materials Science and Engineering
Ohio State University
477 Watta Hall, 2041 College Rd.
Columbus, OH 43210
USA

Dr. Claudine E. Williams
Laboratoire de Physique
CNRS URA 792
Collège de France
11, Place Marcelin Berthélot
F-75231 Paris Cedex 05
France

Contents

The page is intensily left blank

List of Symbols and Abbreviations

a, b, c	crystal unit cell parameters
$\boldsymbol{a}, \boldsymbol{b}, \boldsymbol{c}$	unit cell edge translation vectors
$\boldsymbol{a}^*, \boldsymbol{b}^*, \boldsymbol{c}^*$	reciprocal cell translation vectors
A	sample area
$A(\boldsymbol{q})$	scattering amplitude
b_i	coherent scattering length of atom i
B	bending magnet strength in Tesla (Chapter 2)
B, b	background (Chapter 3)
B, B_{ij}	Debye-Waller temperature factor and tensor components (Chapter 1)
B_i	spin-dependent scattering length of atom i (Chapter 4)
c	solute concentration (Chapter 4)
c	speed of light (Chapter 1)
c	velocity of light (Chapter 2)
C	concentration
d	interplanar spacing (Chapter 3)
d	lattice plane spacing (Chapter 2)
d	sample thickness (Chapter 4)
d_0	Bragg spacing
$\boldsymbol{d}_{hkl}$	interplanar spacing vector
$\boldsymbol{d}^*_{hkl}$	reciprocal cell interplanar spacings
D	particle dimension
$\mathscr{D}$	fractal dimension
e	charge on the electron
$\boldsymbol{e}, \boldsymbol{e}_0$	unit vectors along the diffracted and incident beams
e_i	energy to produce one ion pair
E	energy
E	energy of the beam (Chapter 2)
E_p	energy of the particle
f, f_0	atomic scattering factor
$\Delta f', \Delta f''$	anomalous dispersion scattering components
F	Fano factor
F_{hkl}	structure factor (Chapter 1)
F_i	amplitude of the backscattering factor
F_N	Smith, Synder figure of merit evaluated at line N
F_{nkl}	modulus of the structure factor (Chapter 2)
$g(r)$	radial distribution function
G	Gaussian function
h	Planck's constant
hkl	Miller indices

I	integrated diffracted intensity (Chapter 2)
I	intensity (Chapter 1)
$\boldsymbol{I}$	nuclear spin
I_0	incident intensity (Chapter 1)
I_0	incoming flux (Chapter 2)
$I_{i\alpha}$	intensity of reflection i from phase α
$I(q)$	detector counts
$I(q)$	scattered intensity
I^{rel}	relative intensity, usually on a scale of 100
I_{t}	transmitted flux
$I(\lambda)$	photon intensity
J	total angular momentum
k	magnitude of the photoelectron wave vector (Chapter 2)
$\boldsymbol{k}$	wave vector (magnitude: $2\pi/\lambda$) (Chapter 1)
$\boldsymbol{k}, \boldsymbol{k}_0$	scattering vectors along the diffracted and incident beams (Chapter 4)
K_0	bulk modulus
$\mathrm{K}_{\alpha 1}, \mathrm{K}_{\alpha 2}, \mathrm{K}_{\beta}$	characteristic X-ray emission lines
l	angular quantum number
L	Avogadro's number (Chapter 1)
L	Lorentzian function (Chapter 1)
L	orbital angular momentum (Chapter 3)
L	sample to source distance (Chapter 2)
LLD	lower limit of detection
Lp	Lorentz and polarization corrections
m	magnetic quantum number (Chapter 3)
m	mass
m	sensitivity of X-ray fluorescence method (Chapter 3)
m_0	rest mass of the electron
m_{e}	mass of the electron
M	molecular mass (Chapter 4)
M	multiplicity of a plane (Chapter 1)
M_{20}	de Wolff figure of merit
n	principal quantum number
$n_{\mathrm{b}}, n_{\mathrm{p}}$	number of counts on peak (p) and background (b)
N	number of electrons (Chapter 3)
N	number of measurements (Chapter 3)
N	number of particles in the sample (Chapter 4)
N_{A}	Avogadro's number
N_i	co-ordination number for atoms of type i
$p(r)$	pair-distance distribution function
P	profile due to instrumental effects, the convolution of $W * G$ (Chapter 1)
P, p	peak (Chapter 3)
$P(\boldsymbol{r})$	Patterson function
$P(\lambda)$	photon flux
q	wave vector (magnitude)

q	momentum transfer, $\|q\|=(4\pi/\lambda)\sin\theta$
Q	Porod's invariant
r	real-space distance
r	shell distance
r_i	radial distance from absorbing atom
R	counting rate (Chapter 3)
R	radius of a sphere (Chapter 4)
R	ratio (Chapter 3)
R	refinement factor (Chapter 2)
R	resolution (Chapter 3)
R, r	distance (Chapter 1)
$R(E)$	reflectivity coefficient
R_b, R_p	background and peak counting rates
R_g	geometrical resolution factor in X-ray topography
R_G	radius of gyration
$RIR_{\alpha,\beta}$	reference intensity ratio of phase α with respect to β
R_s	radius of the synchrotron storage ring in meters
R_t	theoretical resolution
s	spin quantum number
s	neutron spin
S	profile from diffraction by the sample (Chapter 1)
S	source size (Chapter 2)
S_0	damping term for multibody effects in EXAFS analysis
S_α	Rietveld scale factor for phase α
t	sample thickness (Chapter 2)
t	time
t_b	background counting time
t_p	peak counting time
T	transmission coefficient
u	root mean square amplitude of vibration
v	partial specific volume
V	accelerating voltage (Chapter 1)
V	irradiated sample volume (Chapter 4)
V	unit cell volume (Chapter 1)
V	voltage (Chapter 3)
V_c	critical excitation potential
V_p	particle volume
W	atomic weight (Chapter 1)
W	weight fraction (Chapter 3)
$W * G$	wavelength and instrumental profiles
x	sample to film distance (Chapter 2)
x	thickness
x, y, z	atomic fractional coordinates
X	weight fraction
z	charge on the nucleus (Chapter 1)

z	number of molecules in the unit cell (Chapter 2)
Z	atomic number (Chapter 3)
Z	number of asymmetric units per unit cell (Chapter 1)
α	total absorption
α, β, γ	cell parameters (Chapter 2)
α, β, γ	interaxial angles (Chapter 1)
$\alpha^*, \beta^*, \gamma^*$	reciprocal cell interaxial angles
β	full width at half maximum of a diffraction peak
$\beta_\varepsilon, \beta_\tau$	peak broadening due to strain and size
$\gamma(r)$	correlation function
Γ	shear gradient
δ	deviation parameter for an incommensurate phase
ε	detector efficiciency (Chapter 4)
ε	residual lattice stress (Chapter 1)
θ	Bragg diffraction angle
2θ	scattering angle
θ_m	diffraction angle of monochromator
Θ	vertical divergence of the beam
Θ_B	Bragg angle
λ	wavelength
λ_c	critical wavelength
λ_d	damping factor used in EXAFS analysis to allow for inelastic scattering effects
λ_{SWL}	short wavelength limit from an X-ray tube
μ	linear absorption coefficient
μ_0	absorption of an atom in the absence of neighbors (Chapter 1)
μ_0	background absorption (Chapter 2)
μ/ϱ	mass absorption coefficient
ν	frequency
$\bar{\nu}$	wave number
ϱ	density
$\varrho(r), \varrho(xyz)$	electron density at location r or xyz
σ	counting error
σ	shielding constant
σ	standard deviation
$d\sigma(q)/d\Omega$	scattering cross section per particle and unit solid angle
$d\Sigma(q)/d\Omega$	macroscopic differential cross section
σ_i	Debye-Waller type factor used in EXAFS analysis (Chapter 2)
σ_i	displacement between absorbing atoms (Chapter 1)
σ_{net}	net counting error
$\sigma_{(N)}$	random error
τ	crystallite size
ϕ	fixed incident glancing angle (Chapter 2)
ϕ	phase angle (Chapter 1)
ϕ	volume fraction occupied by matter (Chapter 4)

ϕ_c	critical angle for total external reflection
Φ_i	phase shift function used in EXAFS analysis
ψ	binding energy (Chapter 3)
ψ	wave function (Chapter 1)
ω	fluorescent yield
$\Delta\Omega$	solid angle subtended by a detection element
χ	EXAFS interference function
$\chi(k)$	EXAFS function
ADP	ammonium dihydrogen phosphate
ASAXS	anomalous small-angle X-ray scattering
b.c.c.	body-centred cubic
BNL/NSLS	Brookhaven National Laboratory National Synchrotron Light Source
CD-ROM	compact disk read only memory
CVD	chemical vapor deposition
DCD	double-crystal diffractometer
EDD	electron diffraction database
EDS	energy dispersive spectroscopy
EDXRD	energy dispersive X-ray diffraction
EISI	elemental and interplanar spacings index
EXAFS	extended X-ray absorption fine structure
f.c.c.	face-centred cubic
FET	field effect transistor
FOM	figure of merit
FWHM	full width at half maximum
ICDD	international centre for diffraction data
IFT	indirect Fourier transformation
ITO	indium/tin oxide
IUPAC	international union of pure and applied chemistry
KZC	K_2ZnCl_4
LSM	layered synthetic micro-structure
MBA-NB	(–)-2-(α-methylbenzylamino)-5-nitropyridine
MBE	molecular beam epitaxy
MCA	multichannel analyzer
ML	monolayers
NF	nickel formate dihydrate
PC	desktop computer
PDF	powder diffraction file
PHA	pulse height analyzer
PIXE	proton excited X-ray fluorescence
PSD	position sensitive detector
PTS	2,4-hexadiynediol-bis-(*p*-toluene sulfonate)
QEXAFS	quick-scanning EXAFS
RDF	radial distribution function
ReflEXAFS	reflectivity EXAFS

SANS	small-angle neutron scattering
SAS	small-angle scattering
SAXS	small-angle X-ray scattering
SR	synchrotron radiation
SSXRF	synchrotron source X-ray fluorescence
TAP	thallium acid phtalate
TEM	transmission electron microscopy
TOF	time of flight
TRXRF	total reflection X-ray fluorescence
WDS	wavelength dispersive spectroscopy
XAS	X-ray absorption spectroscopy
XANES	X-ray absorption near-edge structure
XRD	X-ray diffraction
XRF	X-ray fluorescence
XSW	X-ray standing waves
ZBH	zero background holder

1 X-Ray Diffraction

Robert L. Snyder

Institute for Ceramic Superconductivity, New York State College of Ceramics, Alfred University, Alfred, NY, U.S.A.

1.1 Introduction

X-ray diffraction has acted as the cornerstone of twentieth century science. Its development has catalyzed the developments of all of the rest of solid state science and much of our understanding of chemical bonding. This article presents all of the necessary background to understand the applications of X-ray analysis to materials science. The applications of X-rays to materials characterization will be emphasized, with particular attention to the modern, computer assisted, approach to these methods.

1.2 The Nature of X-Rays

X-rays are relatively short wavelength, high energy electromagnetic radiation. When viewed as a wave we think of it as a sinusoidal oscillating electric field with, at right angles, a similar varying magnetic field changing with time. The other description is that of a particle of energy called a photon. All electromagnetic radiation is characterized by either its energy E, wavelength λ (i.e., the distance between peaks) or its frequency ν (the number of peaks which pass a point per second). The following are useful relationships for interconverting the most common measures of radiation energy.

$$\lambda = \frac{c}{\nu} \tag{1-1}$$

$$E = h\nu \tag{1-2}$$

where c is the speed of light and h is Planck's constant. Spectroscopists commonly use wavenumbers particularly in the low energy regions of the electromagnetic spectrum, like the microwave and infrared. A wave number ($\bar{\nu}$) is frequency divided by the speed of light

$$\bar{\nu} = \frac{\nu}{c} = \frac{c/\lambda}{c} = \frac{1}{\lambda} \tag{1-3}$$

The angstrom (Å) unit, defined as 1×10^{-10} m, is the most common unit of measure for X-rays but the last IUPAC vention made the nanometer (1×10^{-9} m) a standard. However, here we will use the traditional angstrom unit. Energy in electron volts (eV) is related to angstroms through the formula,

$$E(\text{eV}) = \frac{hc}{\lambda_{\text{cm}}} = \frac{12\,396}{\lambda_{\text{Å}}} \tag{1-4}$$

Electron volts are also not IUPAC approved in that the standard energy unit is the Joule which may be converted by

$$1\ \text{eV} = 1.602 \times 10^{-19}\ \text{J} \tag{1-5}$$

It should be noted that despite the IUPAC convention, Joules are never used by crystallographers or spectroscopists, while a few workers have adopted the nanometer in place of the angstrom. Table 1-1 lists the various measures across the electromagnetic spectrum.

1.3 The Production of X-Rays

There are four basic mechanisms in nature which generate X-rays. These are related to the four fundamental forces that exist in our universe. Any force when applied to an object is a potential source of energy. If the object moves kinetic energy is generated. The weak and strong nuclear forces combine to produce not very useful X-rays, along with many other wavelengths and subatomic particles, in high energy nuclear collisions. The force of gravitation also produces X-rays which are not useful in the materials characterization

Table 1-1. Values of common energy units across the electromagnetic spectrum.

Quantity	Units	IR	UV	Vacuum UV	Soft X-ray	X-ray	Hard X-ray	γ
Wavelength	Å	10000	1000	100	10	1	0.1	0.01
Wavelength	nm	1000	100	10	1	0.1	0.01	0.001
Wavenumber	cm^{-1}	10^4	10^5	10^6	10^7	10^8	10^9	10^{10}
Energy	eV	1.24	12.4	124	1239.6	12.4 keV	124 keV	1.24 MeV
Energy	J	2×10^{-19}	2×10^{-18}	2×10^{-17}	2×10^{-16}	2×10^{-15}	2×10^{-14}	2×10^{-13}

laboratory, by giving rise to neutron stars and black holes which, in the process of accreting matter, produce X-rays visible at astronomical distances. However, it is the Coulombic force which produces the X-rays we harness in the laboratory.

1.3.1 Synchrotron Radiation

Particle accelerators operate on the principle that as a charged particle passes through a magnetic field it will experience a force perpendicular to the direction of motion, in the direction of the field. This causes a particle to curve through a "bending magnetic" and accelerate. As long as energy is supplied to the magnets, a beam of particles can be continuously accelerated around a closed loop. Accelerating (and decelerating) charged particles will give off electromagnetic radiation. When the particles are accelerated into the GeV range, X-radiation will be produced. A synchrotron is a particle acceleration device which, through the use of bending magnetics, causes a charged particle beam to travel in a circular (actually polyhedral) path.

Today there are a number of synchrotron facilities around the world which are dedicated to the production of extremely intense sources of continuous (white) X-radiation ranging from hundredths to hundreds of angstroms in wavelength. In recent years there has been a burst of activity in the use of these sources. The wavelength tunability and very high brightness of these sources has opened a wide range of new characterization procedures to researchers. The addition of magnetic devices to make the particle beam wiggle up and down on its path between bending magnetics, called wigglers and undulators, have raised the intensity of X-rays available for experiments by as much as a factor of 10^{12}. In addition, since the X-rays are only produced as the charged particles fly by the experimenter's window every few nanoseconds, time-resolved studies in the nanosecond range have become accessible. See the chapter on synchrotron radiation by Sherwood et al. in this volume for more information on synchrotron techniques.

1.3.2 The Modern X-Ray Tube

The conventional method of producing X-rays in a laboratory is to use an evacuated tube invented by Coolidge (1913). Figure 1-1 shows a modern version of this tube whose function is illustrated in Fig. 1-2. This tube contains a tungsten cathode filament which is heated by an AC voltage ranging from 5 to 15 V. The anode is a water-cooled target made from a wide range of pure elements. Electrons are accelerated in vacuum under potentials of 5000 to 80 000 volts and produce a spectrum of the type shown in Fig. 1-3. As the accelerated electrons reach the target they are re-

pelled by the electrons of the target atoms, causing a slowing down or breaking. To slow down an electron and conserve energy, the electron must lose its energy in the only manner available to it – radiation. The German word for breaking is brems and for radiation is strahlung. Most of the early discoveries concerning X-rays oc-

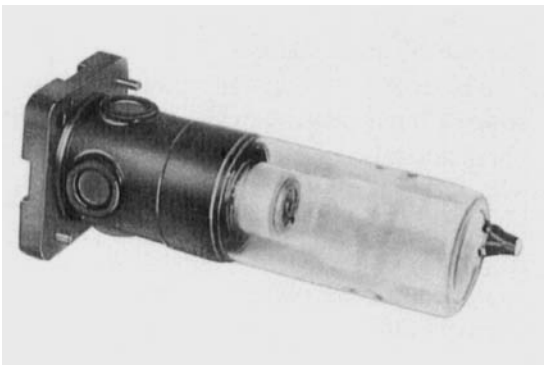

Figure 1-1. The modern sealed X-ray tube (Courtesy of Siemens AG).

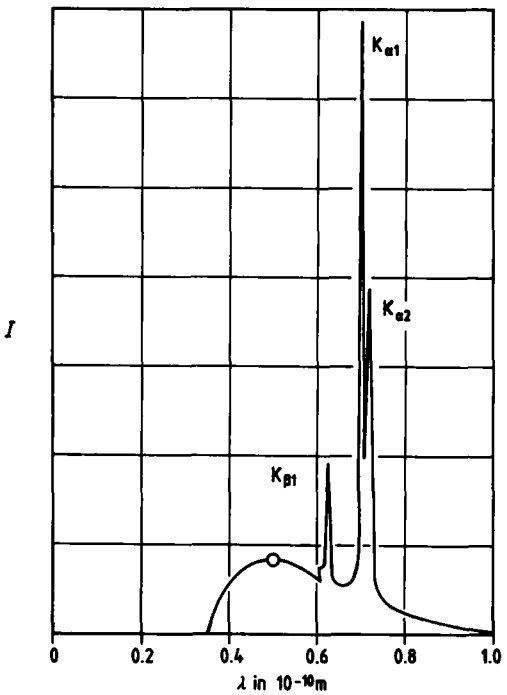

Figure 1-3. The spectrum from a Mo target X-ray tube.

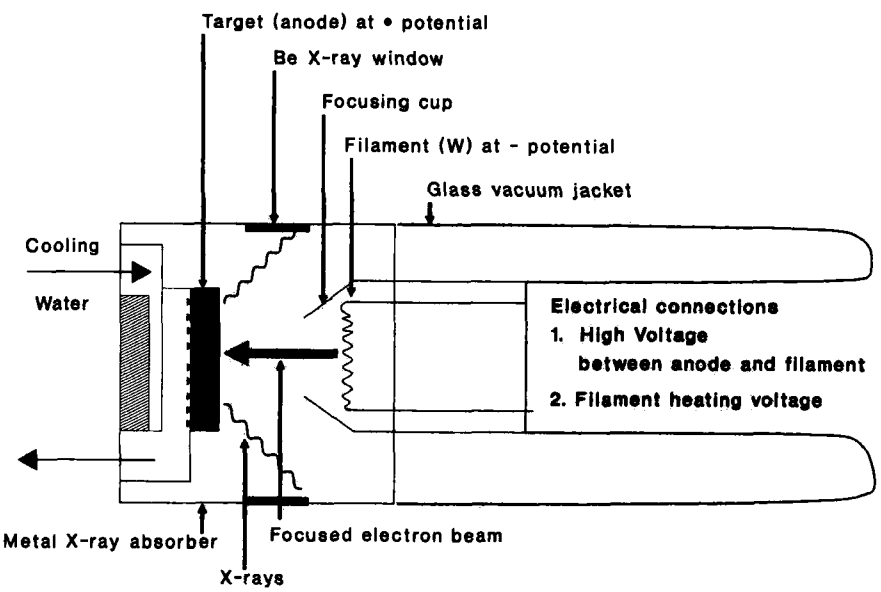

Figure 1-2. Schematic of an X-ray tube.
$(\lambda) = \mathrm{m}$, $(\nu) = (c/\lambda) = \mathrm{s}^{-1}$, $(h\nu) = (E) = \mathrm{eV}$,
$(c) = \mathrm{m/s}$, $(E) = \mathrm{J}$ or eV, $\left(h\frac{c}{\lambda}\right) = \mathrm{eV}$, $(hc) = \mathrm{eV \cdot m}$,
$(hc)/\mathrm{eV} = \mathrm{m} = (\lambda)$.

curred in Germany; for example, Röntgen, the discoverer of X-rays, worked at the University of Munich (although the discovery was actually made in Würzburg), where others like von Laue and Ewald were to make dramatic advances. Since Germans seem to have a running competition to form the world's longest words, they called this continuous spectrum *bremsstrahlung*; which we have adopted as a rather odd sounding English word.

The maximum energy of a photon from such an X-ray tube would arise from a single dead stop collision of an accelerated electron with a target electron. The kinetic energy of the electron is the product of e and V, where e is the charge on the electron and V is the accelerating voltage. If this energy is completely converted to a photon of energy $h\nu$ then the *short wavelength limit* (λ_{SWL}) of the photons in the continuous spectrum will be

$$\lambda_{SWL}(\text{Å}) = hc/(eV) = 12\,398/\text{V} \qquad (1\text{-}6)$$

Superimposed on the white radiation from an X-ray tube are some very narrow spikes. The wavelengths of these lines were first shown by Moseley to be a function of the atomic number of the target material. They arise from billiard ball like collisions which eject inner shell electrons from the target atoms. This process is described more fully below. It should be noted that it makes no difference whether an inner shell "photoelectron" is ejected by an electron, as in an X-ray tube or, by a photon as in an X-ray spectrometer, the resulting emission lines will be the same. It is these nearly monochromatic emission lines which we employ for most of our X-ray experiments.

1.3.3 High Intensity Laboratory X-Ray Devices

The conventional modern X-ray tube uses a cup around the tungsten filament held at a potential of a few hundred volts more negative than the cathode so that the electrons are repelled and focused onto the target. The focal spot is actually a line about two centimeters in length, reflecting the length of the filament. Intensity is defined as the photon flux passing a unit area in unit time. Thus, focusing the electrons onto a smaller area increases the intensity. Various modifications of design parameters have produced "fine focus" and "long fine focus" X-ray tubes which take advantage of this fact to produce higher intensity. However, approximately 98% of the energy from the impacting electrons goes into producing heat. The limitation on the intensity which may be produced is the efficiency of the cooling system which prevents the target from melting.

Since the X-rays may be viewed from any of the four sides of the tube, two sides will produce X-rays from the line projection of the filament. The other two sides view the projection of the line from the end giving a focal spot (actually a rhombus) of about 1 mm^2 in size, when viewed from the usual take-off angle of from 3° to 6°. The take-off angle is the angle at which an experiment views the X-ray tube target. The higher the angle the more divergent X-rays will be present and the lower will be the resolution of any experiment. On the other hand, decreasing the angle decreases intensity but, by limiting the amount of angular divergence in the beam, increases the experimental resolution.

Microfocus tubes use the focusing cup to squeeze the electron beam down to a spot focus with a diameter as small as 10 μm. These units are used for experiments requiring extremely intense beams and can accept the small area of illumination. Such tubes usually have replaceable targets. Another, more popular, method to increase the intensity of an X-ray tube is to increase

the power on the target and avoid melting it by rotating it. These rotating anode tubes continuously bring cool metal into the path of the focused electron beam. Such units can typically be run as high as 18 kW compared to about 1.8 kW for a sealed tube. They produce very intense X-ray beams. However, owing to the mechanical difficulties of a high speed motor drive which must feed through into the vacuum, there are difficulties in routine continuous operation. In recent years these units have become more common and more reliable.

The last laboratory method for generating X-rays is to charge a very large bank of capacitors and to dump the charge, in a very short time, to a target. These *flash X-ray* devices can reach peak currents of 5000 A in the hundreds of kV range. The extremely intense X-ray flash lasts for only a few nanoseconds but this has not stopped workers from performing some very clever experiments within this incredibly small time window.

1.4 Interaction of X-Rays with Matter

Consider the simple experimental arrangement shown in Fig. 1-4. Any mechanism which causes a photon, in the collimated incident X-ray beam, to miss the detector is called absorption. Most of the mechanisms of absorption involve the conversion of the photon's energy to another form; while some simply change the photon's direction. For the purposes of this discussion it is best to consider I_0 a monochromatic beam and that the detector is set only to detect X-rays of that energy. We may place the possible fates of an X-ray photon, as is passes through matter, in the following categories.

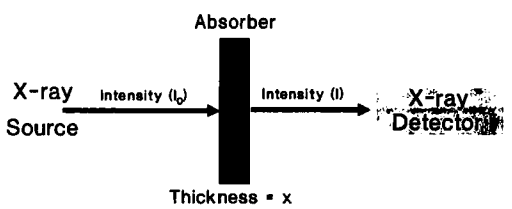

Figure 1-4. A simple absorption experiment.

1.4.1 No Interaction

The fundamental reason for all X-ray–atom interactions is the acceleration experienced by an atom-bound electron from the oscillating electric field of the X-ray's electromagnetic wave. The probability of any interaction decreases as the energy of the wave increases. The probability of interaction is approximately proportional to the wavelength cubed. Thus, short wavelength photons are very penetrating while long wavelengths are readily absorbed. There is always a finite probability that an X-ray will pass through matter without interaction.

The simple cubic relationship of interaction probability is disturbed by the phenomenon of *resonance absorption.* When the energy of the incident radiation becomes exactly equal to the energy of a quantum allowed electron transition between two atomic states, a large increase is observed in the probability of a photon's being absorbed. The dramatic increase in absorption as photons reach the ionization potential of each of the electrons in an atom results in a series of absorption edges shown in Fig. 1-8.

1.4.2 Conversion To Heat

Heat is a measure of atomic motion. Heat may be stored in the quantum allowed translational, rotational and vibrational energy states of the atoms or molecules in a material. It also can be stored in the various excited electronic

states allowed to an atom and in the motion of the relatively free electrons in metals. The principal mechanism for converting photons to heat in insulators is the stimulation of any of the modes of vibration of the lattice.

There are two classes of vibrational modes allowed to any lattice. One is the acoustic modes of vibration which may be stimulated by a mechanical force such as a blow or an incident sound wave. The other class is the optic modes of vibration. Optic modes are characterized by a change in dipole moment as the atoms vibrate. This change in electrical field in the lattice allows these modes to interact with the electric field of a photon. Thus, an X-ray photon may stimulate an optic lattice vibrational mode which we observe as heat. The efficiency of the coupling between the lattice vibrational modes, called phonons, and photons, depends both on the lattice itself and on the energy of the incident photon. Thus, we observe sample heating in an X-ray beam to be higher in some samples than in others.

In fact X-rays can also gain energy by absorbing a phonon. The energy of the lattice vibrational modes is on the order of 0.025 eV, while a Cu K_α photon has an energy of 8 keV. Thus, the modification of the incident X-ray beam is rather small, and of course can be studied to understand the phonon structures of solids. However, Raman spectroscopy and thermal neutron scattering are better for these types of studies. Photons whose energy has been modified by a phonon interaction contribute to experimental background as thermal diffuse sacttering.

1.4.3 Photoelectric Effect

In a photon–electron interaction, if the photon's energy is equal to, or greater than, the energy binding the electron to the nucleus, the electron may absorb all of the energy of the photon and become ionized as shown in Fig. 1-5. The free electron will leave the atom with a kinetic energy equal to the difference between the energy of the incident photon and the ionization potential of the electron. This high energy electron can, of course, go on to initiate a number of photon creating events. However, any secondary photon must have a lower energy. The experiment illustrated in Fig. 1-4 assumes that the detector is set only to count pulses of the same energy as in the incident monochromatic beam. Thus, these secondary or fluoresced photons of lower energy do not get included in the measurement of intensity.

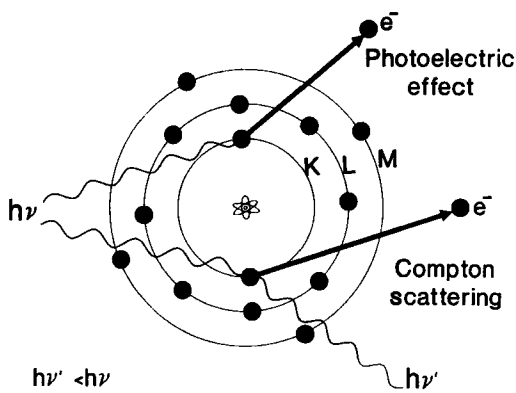

Figure 1-5. Photoelectric and Compton effects.

1.4.3.1 Fluorescence

An atom, ionized by having lost one of its innermost K or L shell electrons, is left in an extremely unstable energy state. If the vacancy has occurred in any orbital beneath the valence shell, then an immediate rearrangement of the electrons in all of the orbitals above the vacancy will occur. Electrons from higher orbitals will cascade down to fill in the hole. This process, illustrated in Fig. 1-6, causes the emission of

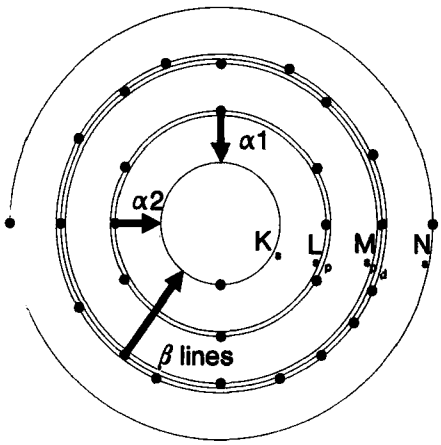

Figure 1-6. Fluorescence from an ionized atom.

secondary fluorescent photons. The energy gaps between the various electron orbitals are fixed by the laws of quantum mechanics. Thus, the photon emitted by an electron falling to lower energy (getting closer to the nucleus) will have a fixed energy, depending only on the number of protons in the nucleus. The photons fluoresced by any element will thus have X-ray wavelengths characteristic of that element.

If the ionized electron comes from the K shell, then there is a certain probability that an L_p, L_s or an M electron will fall in to replace it. The names of the resulting emitted photons are the $K_{\alpha 1}$, $K_{\alpha 2}$ and K_β, respectively. For a Cu atom the transition probabilities are roughly 5:2.5:1, respectively. The energies of any of these lines must, of course, be less than that of the original incident X-ray which caused the ionization. The study of the fluoresced photons is called X-ray fluorescence spectroscopy (XRF). This technique allows the rapid qualitative analysis of the elements present in a material and with more work, the quantitative analysis of the elemental composition. See Chap. 3 for a complete description of this method.

1.4.3.2 Auger Electron Production

There is a special tertiary effect of photoelectron production called the emission of Auger (pronounced oh-jay) electrons. Sometimes the removal of an inner-shell electron produces a photon which in turn gets absorbed by an outer-shell, valence electron. Thus, the incident X-ray gets absorbed by, for example, a K shell electron which leaves the atom. An L shell electron can fall to the K shell to fill in the hole and thereby causes the emission of a K_α X-ray photon. However, before this photon can leave the atom it gets absorbed by a valence electron which ionizes and flies off leaving a doubly charged ion behind. This process is illustrated in Fig. 1-7.

The kinetic energy of the Auger electron is not dependent on the energy of the initial X-ray photon which ionized the K electron. Any X-ray with sufficient energy to create the initial K hole can be responsible for the subsequent production of an Auger electron of fixed kinetic energy. This very specific kinetic energy is equal to the difference in energy between the fixed-energy K_α or K_β photon which ionized the Auger

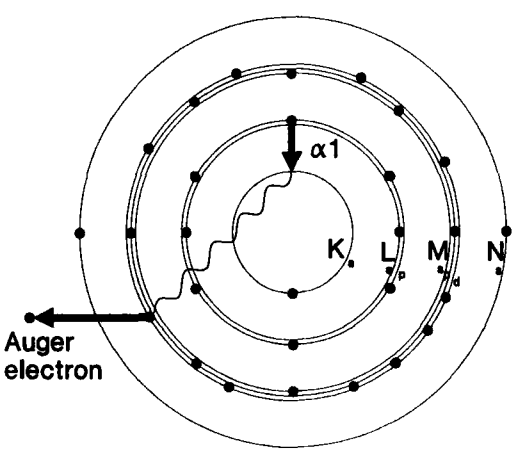

Figure 1-7. Auger electron emission from an ionized atom.